Hindawi
International Transactions on Electrical Energy Systems
Volume 2024, Article ID 5541124, 17 pages
https://doi.org/10.1155/2024/5541124

Research Article

A Novel Design and Analysis Adaptive Hybrid ANFIS MPPT Controller for PEMFC-Fed EV Systems

Ezzeddine Touti,[1,2] **Mouloud Aoudia**,[3] **C. H. Hussaian Basha**,[4] **and Ibrahim Mohammed Alrougy**[5]

[1]*Department of Electrical Engineering, College of Engineering, Northern Border University, Arar 91431, Saudi Arabia*
[2]*Department of Electrical Engineering, Higher Institute of Applied Sciences and Technology of Kasserine, University of Kairouan, Kairouan 3100, Tunisia*
[3]*Department of Industrial Engineering, College of Engineering, Northern Border University, Arar 91431, Saudi Arabia*
[4]*Electric Vehicle R&D Lab, Nitte Meenakshi Institute of Technology, Bangalore, India*
[5]*King Abdulaziz City for Science and Technology (KACST), Riyadh, Saudi Arabia*

Correspondence should be addressed to Mouloud Aoudia; mouloud.aoudia@nbu.edu.sa and C. H. Hussaian Basha; hussaian.basha@nmit.ac.in

Received 8 February 2024; Revised 17 March 2024; Accepted 25 March 2024; Published 9 April 2024

Academic Editor: Adel Oubelaid

Copyright © 2024 Ezzeddine Touti et al. This is an open access article distributed under the Creative Commons Attribution License, which permits unrestricted use, distribution, and reproduction in any medium, provided the original work is properly cited.

Now, the present electric vehicle industry is focusing on the fuel cell technology because its features are high flexibility, continuous power supply, less atmospheric pollution, fast startup, and rapid response. However, the fuel cell gives nonlinear power versus current characteristics. Due to this nonlinear behavior, the maximum power extraction from the fuel stack is quite difficult. So, in this work, an adaptive genetic algorithm with an adaptive neuro-fuzzy inference system (ACS with ANFIS) MPPT controller is introduced for finding the MPP of the fuel stack system thereby extracting the peak power from the fuel stack. The proposed hybrid maximum power point tracking (MPPT) controller is compared with the other MPPT controllers which are enhanced incremental conductance-fuzzy logic controller (EIC with FLC), improved hill climb with fuzzy logic controller (IHC with FLC), adaptive beta with FLC, enhanced differential evolutionary with FLC (EDE with FLC), and marine predators optimization with FLC (MPO with FLC). Here, these hybrid controllers' comprehensive investigations have been carried out in terms of tracking speed of the MPP, oscillations across the MPP, settling time of the converter voltage, maximum power extraction from the fuel stack, and working efficiency of the MPPT controller. The fuel stack generates a very low output voltage which is improved by using the boost DC-DC converter, and the overall fuel stack-fed boost converter system is designed by utilizing the MATLAB/Simulink tool. From the simulation results, the AGA with ANFIS MPPT controller gives high MPP tracking efficiency when compared to the other hybrid controller.

1. Introduction

From the current research trend, most of the nonrenewable sources' utilization keeps on reducing because of their demerits are high installation cost, need for high catchment area for the establishment, high greenhouse gas emissions, high impact on human health, and low reliability. Due to these drawbacks, most of the electric vehicle industries focus on renewable energy systems which are tidal, wind, solar, and hydropower systems [1]. In article [2], the authors discussed the tidal power supply system. Here, at the high tide period, the water flows from the sea into a water turbine to generate electricity for the local consumers. In this system, the height of the tide is high, and then, the power generation from the tidal system is high. Otherwise, the power output from the tidal network is low. The features of tidal power supply systems are environmentally friendly, predictable energy, high power density, and less operational and

maintenance cost [3]. The disadvantages of tidal systems are high construction cost, the formation of silt behind the barrage, and the high effect on animals and plants that are living near the tidal power systems. So, the tidal power systems' drawbacks are limited by using solar photovoltaic (PV) power systems [4].

Most of the solar cells are manufactured by using the monocrystalline silicon material because of their high operating efficiency. The operation of solar cells is similar to the P-N diode, and these cells are interconnected in series to improve the overall supply voltage of the solar system [5]. Similarly, the solar cells are connected in parallel to increase the current rating of the PV array. However, the drawbacks of solar systems are high installation costs, highly expensive storage, continuous dependence on sunlight energy, and less operating efficiency [6]. Also, the solar systems give discontinuous power supply because the sunlight energy varies from time to time. So, the wind energy power system is used [7] to limit the drawbacks of solar PV. In a wind power generation system, the wind energy is converted into rotational energy. Finally, the rotational energy is transferred into the electrical power supply by using the three-phase generators. The advantages of wind energy systems are inexhaustible, not pollutant, reduced fossil fuel utilization, and created wealth and local employment [8]. The disadvantages of wind systems are high noise creation and affect the wildlife. However, the limitations of all renewable energy sources are overcome by using fuel cell technology [9]. At present, fuel cell power generation is playing a major predominant role in electric vehicle systems because its merits are less dependency on nature, continuous electricity supply, very low environmental pollution, and more flexibility [10].

From the current literature review, the fuel stacks are classified as molten carbonate fuel stack (MCFS), solid oxide fuel stack (SOFS), phosphoric acid fuel stack (PAFS), alkaline fuel stack (AFS), direct methanol fuel stack (DMFS), and zinc-air fuel stack (ZAFS). In [11], the authors utilized the MCFS in the steel industry applications for capturing the entire hydrogen. Here, the molten carbonate material is used as an electrolyte in the MCFS. The operating principle of MCFS is the indirect combination of oxygen, and hydrogen has been carried out in the presence of water to generate the electrical power supply. The features of MCFS are high operating temperature capability which is nearly equal to 650°C, good dynamic response, high functioning efficiency, and more fuel flexibility [12]. However, the MCFS is not suitable for portable applications. In addition, this fuel stack lifetime is reduced when the operating temperature is increased. The demand for fuel stack is shown in Figure 1. The limitations of MCFS are overcome by using the SOFS [13]. All the SOFSs work at high operating temperatures with high efficiency. Also, the SOFS does not require any external reformers because the gas fuel is reformed within the fuel cell. In this stack, the solid oxide material is used as an electrolyte for transferring the hydrogen ions from the anode to the cathode. The features of SOFS when compared to the traditional power conversion systems are more reliability, high temperature withstand ability, good reliability, and fuel adaptability. Moreover, this fuel cell releases very low levels

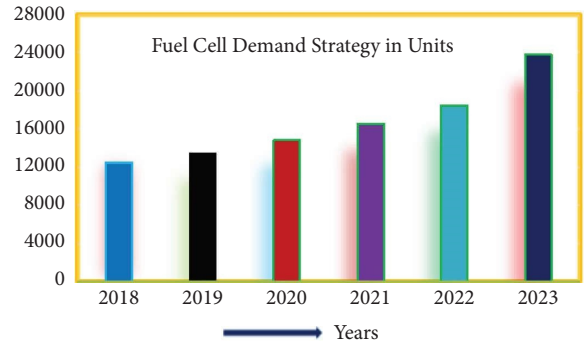

Figure 1: Present strategy of fuel cell demand in units.

of nitrous oxide and solid oxide gasses [14]. So, the overall environmental pollution is reduced extensively. Also, the solid oxide fuel stacks are used for auxiliary power supply and distribution power generation systems. The disadvantages of SOFS are longer startup time and high mechanical and chemical compatibility problems. Also, this fuel stack is suffering from different degradation-related issues.

So, in [15], the authors implemented the phosphoric acid fuel stacks for hospital and commercial household heating systems. Here, the liquid-type electrolyte is used, and the catalyst is designed by utilizing platinum material. The maximum working efficiency of the PAFS is between 38% and 40%. The major advantages of PAFS are high reliability, more flexibility, and cogenerated heat [16]. Also, this fuel stack produces very low environmental pollutants. However, the disadvantages of PAFS are less power density, high sensitivity to the fuel quality, very low startup time, high design complexity, and higher manufacturing cost. Most of the DMFSs are used for domestic and electric vehicle transportation applications. In this cell, the methanol material is utilized as an electrolyte for transferring the electrons from the anode layer to the cathode layer. The features of this fuel cell are more efficiency, the ability to operate at very low temperatures, high portability, and very less hazardous gas emissions [17]. However, output water management is very difficult in this fuel stack. Also, the cost of the catalyst in this fuel stack is very high. The zinc-air fuel stack is used for hospitalized stationary applications, and its electrochemical reaction happens between the zinc and oxygen for generating the electricity in the automotive systems [18]. The features of this fuel stack are lightweight design, environmentally friendly, long lifetime period, low self-discharge rate, high scalability, and more compact in design [19]. The disadvantages of this fuel stack are high complexity in recharging and high internal short circuits, and the handling of electrolytes in the fuel stack at high operating temperatures is very difficult.

So, the above fuel stack's drawbacks are limited by using the PEMFS. The features of the PEMFS are high robustness, more flexibility, good dynamic response, less steady-state voltage oscillations, and high operating efficiency. The proposed fuel stack-fed boost converter system is given in Figure 2. However, the PEMFS gives nonlinear power versus voltage characteristics. So, the peak voltage extraction from

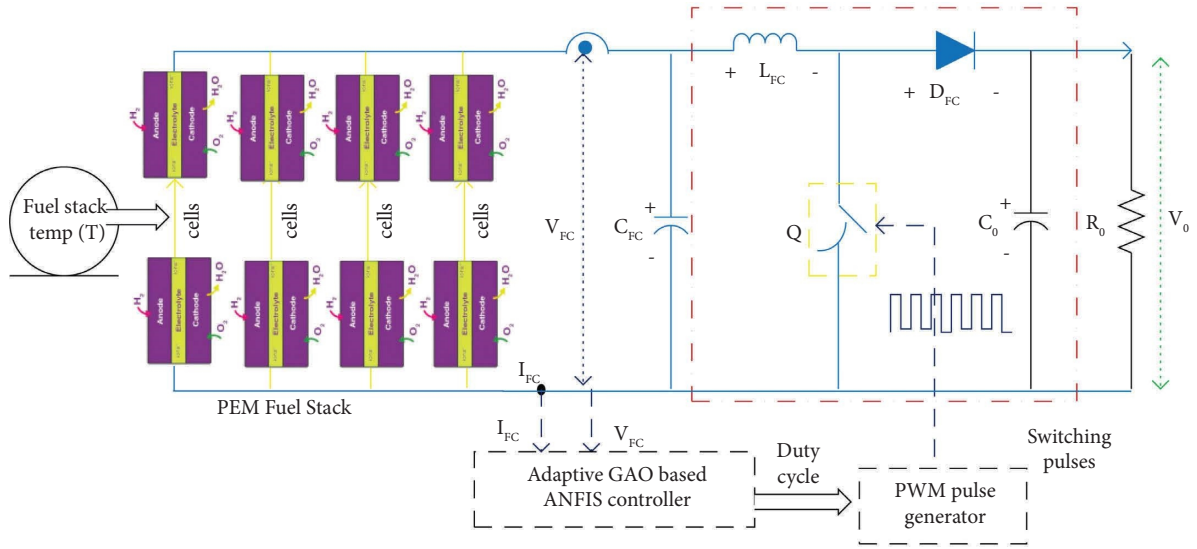

Figure 2: Proposed adaptive genetic algorithm-optimized ANFIS-fed fuel stack system.

the PEMFS is a difficult task. In [20], there are various types of MPPT methodologies are utilized for finding the operating point of the fuel stack. The fundamental categories of power point tracking controllers are soft computing, evolutionary, nature-inspired, and artificial intelligence-based MPPT controllers. In addition, there are three more types of MPPT controllers available which are offline, online, and hybrid MPPT controllers [21–23]. The most frequently used online MPPT controllers are Perturb & Observe (P&O), Hill Climb (HC), Incremental Conductance (IC), Kalman filter, ripple correlation controller, and Incremental Resistance MPPT controller. In this P&O controller, the functioning point of the fuel stack is operated at the peak power point by using the slope of the voltage versus current characteristics. The present evaluated slope value consists of a positive indication, and then, the slope of the V-I curve is increased thereby enhancing the duty value of the boost converter. Otherwise, the duty cycle of the boost converter is reduced to move the functioning point of the fuel stack near the actual MPP position. The merits of this conventional online controller are easy design, less complexity in implementation, more flexibility, easy handling, and good static response of the system. However, this controller gives high oscillations across the functioning point of the fuel stack [24].

So, the P&O controller drawbacks are compensated by integrating the IC MPPT controller along with the PEMFS system. In this controller, the MPP tracking of the PEMFS has been carried out by varying the equivalent conductance of the fuel cell. Here, the functioning point of the PEMFS is at the right side of the V-I curve, and then, the equivalent conductance value is increased. Otherwise, the conductance of the system is reduced for optimizing the oscillations across MPP [25–28]. All the renewable energy-fed power electronics circuits generate ripples which are supplied to the ripple correlation block to generate the suitable duty signal to the DC-DC converter [29–32]. Due to this controller operation, the fuel stack system power conduction losses are reduced, and the entire system size is reduced. However, this ripple correlation controller is less applicable to the dynamic operating temperature conditions of the fuel stack. In [33], the authors introduced the incremental resistance methodology for finding the operating point of the fuel stack at various water membrane conditions. Here, the current density function is used for identifying the MPP position of the fuel stack. The merits of this controller are simple in design, easy handling, less complexity in understanding, and less implementation cost. However, this conventional controller is used where the accuracy of the MPPT controller is not needed.

The slider concept is used in [34] for improving the accuracy of MPP tracking at different water membrane conditions. In this slider method, state space analysis is used to find the boundary conditions of the MPPT controller. The slider MPPT controller features are more flexibility, high efficiency, and high robustness for various operating temperature conditions of the SOFS. The disadvantages of this controller are more settling time of the converter output voltage and the need for more installation area [35]. So, an artificial neural network (ANN) is used in the PV/PEMFS system for optimizing the overall system size and generating the proper duty signal to the bidirectional two-phase DC-DC converter. The ANNs are implemented by utilizing the human brain behavior and its nervous system. Here, the ANNs need less mathematical computations and are easy to handle complex nonlinear problems. The demerits of ANN are lack of transparency in decision-making, potential overfitting without proper regularization, limited expressive power, and generalization ability [36–39]. So, the drawbacks of ANN are limited by using the fuzzy logic system in the hybrid PV/wind/SOFS system. Fuzzy is a type of mathematical system that analyses the analog parameters in terms of logical variables. The fuzzy system consists of three blocks which are fuzzification, defuzzification, and inference block. The fuzzification block is used to convert the crisp values into fuzzy sets. The defuzzification block is used to convert

fuzzy sets into crisp values. The features of fuzzy controllers are less cost to implement and easy to understand because of the absence of mathematical calculations [40].

The drawbacks of fuzzy systems are less accuracy in MPP tracking and more oscillations across the MPP [41]. So, the adaptive neuro-based fuzzy inference system (ANFIS) is used in the article [42] to overcome the disadvantages of fuzzy logic controllers. The ANFIS controller is designed from the merits of ANN and fuzzy controllers. Here, this controller takes the fuel stack operating temperature, converter input voltage, water membrane content, converter input current, and hydrogen decomposition to generate the switching pulses to the DC-DC converter. The features of the ANFIS controller are high MPP tracking accuracy, moderate converter voltage ripples, and good dynamic response. However, it needed more convergence time for tracking the MPP of the fuel stack [43–46]. So, the particle swarm optimization (PSO)-based MPPT methodology is utilized in the fuel stack single-stage inverter system for reducing the convergence time of the MPP. Here, at the beginning stage of the PSO operation, all the particles move with different velocities and different directions in the entire search space. After completion of a certain number of iterations, most of the particles move towards the required object. Here, the PSO controller may not give the exact position of the fuel stack MPP when the total number of iterations is increased extensively. So, in this article, an adaptive genetic algorithm with an adaptive neuro-fuzzy inference system (ACS with ANFIS) MPPT controller is introduced to generate a suitable duty cycle for the DC-DC converter.

From the literature review, most of the fuel cells' voltage generation is very low which is not useful for electric vehicle applications. So, a boost DC-DC converter is integrated with the EV-fed PEM fuel stack system to enhance the voltage supply rating of the fuel stack. In [47], the researchers discussed the various categories of power converters which are nonisolated and isolated DC-DC boost converters. The isolated power converters are flyback and forward. In both of these converters, there is an electrical barrier between the supply and load of the converter. Due to this barrier, the power semiconductors work efficiently without any damage. However, these isolated converters need an additional transformer and rectifier for stepping up the fuel stack output voltage. As a result, the implementation cost is increased, and the overall circuit complexity is increased [48]. So, the present power electronic converter designers are focusing on nonisolated DC-DC converters for electric vehicle applications. In this work, a conventional power converter is used to enhance the voltage profile of the fuel stack. The features of this selected boost converter are easy to design, and fewer components are required for implementation, easy understanding, and less maintenance cost. The remaining part of the article is organized as follows: the mathematical design of the proton exchange membrane fuel cell and its related functioning characteristics are illustrated in Section 2. In Section 3, the design and performance investigation of various hybrid maximum power point tracking controllers has been carried out. Sections 4 and 5 give the selected conventional DC-DC converter design and simulation results of the fuel stack-fed DC-DC converter system under various operating temperature conditions of the fuel stack. Finally, Section 6 illustrates the conclusion of the article.

2. Design and Implementation of PEM Fuel Cell

From the literature study, most of the renewable energy sources give nonlinear power with high-level distortions. Also, the solar, wind, and tidal power generation systems may not give efficient continuous power to the electric vehicle systems. So, most of the present electric vehicle manufacturing industries are focusing on fuel cell technology because its attractive features are more reliability, high continuity in power supply, high robustness, and releases less environmental pollutants [49]. From Section 1, there are different types of fuel cell technologies are seen and which have their advantages and disadvantages. Here, in this work, the proton exchange membrane fuel cell is used for efficient power supply to the electric vehicle system. The merits of PEMFC are fast startup and the ability to operate at very low temperatures. Also, the handling of PEMFC is very easy because it does not have any rotating parts to generate noise pollution. Moreover, the PEMFC requires less maintenance cost. The disadvantages of PEMFC are highly expensive and require more implementation costs. The overall operation of the PEMFC is given in Figure 3(a), and its related working circuit is given in Figure 3(b).

From Figure 3(a), the fuel cell input sources are hydrogen and oxygen, and those are fed to the anode and a cathode to the PEMFC. The fuel stack-generated nonlinear V-I curve is shown in Figure 4. The PEMFC design parameters are given in Table 1. Here, the H_2 is splitting into ions to release the electrons that are collected at the external load circuit. At the cathode, the water is obtained which is recycled to generate the hydrogen. The chemical reactions of PEMFC are derived as follows:

$$\mathrm{H_2} \Longrightarrow 2\mathrm{H^+} + 2\mathrm{e^-} \tag{1}$$

$$2\mathrm{H^+} + 2\mathrm{e^-} + \frac{1}{2}\,\mathrm{O_2} \Longrightarrow \mathrm{H_2O} \tag{2}$$

$$\mathrm{H_2} + \frac{1}{2}\,\mathrm{O_2} \Longrightarrow \mathrm{H_2O} + \text{energy} \tag{3}$$

From equations (1) and (2), the electricity generated from the single cell (E_{FC}) is not useful. So, there are multiple fuel cells (n) that are interfaced with each other in order to enhance the supply voltage. The entire fuel stack voltage (E_{Total}) generation is determined as follows:

$$E_{\mathrm{Total}} = n * E_{\mathrm{FC}}, \tag{4}$$

$$V_{\mathrm{FC}} = E_{\mathrm{Octv}} - V_O - V_A - V_C, \tag{5}$$

$$\begin{aligned} E_{\mathrm{Octv}} &= 1.29 - 0.8e^{-3} * \left(T_F - 298.12\right) \\ &\quad + 4.3e^{-5} \log\left(P_{H_2}\sqrt{P_{O_2}}\right) T_F, \end{aligned} \tag{6}$$

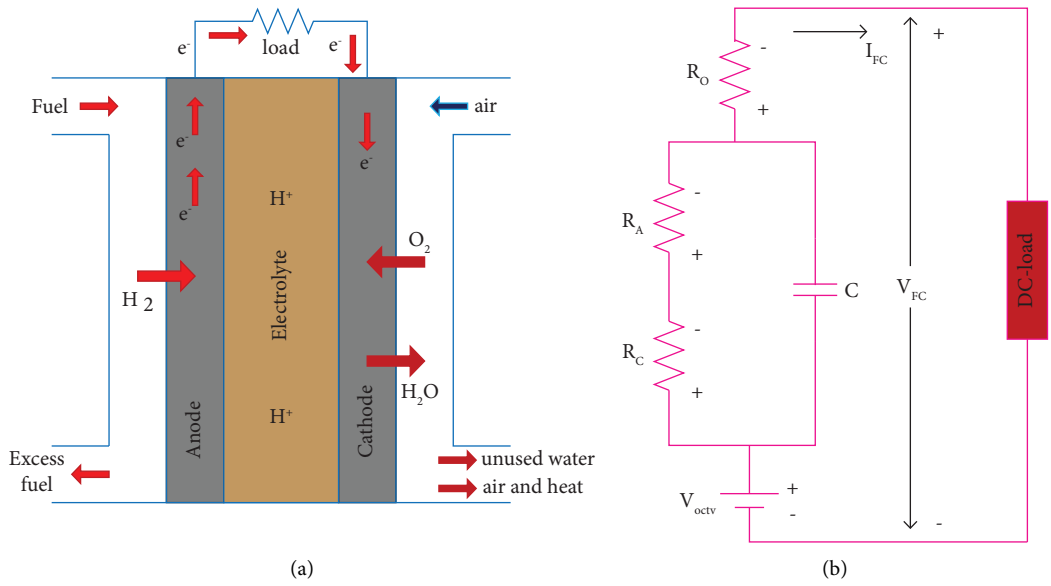

Figure 3: (a) Working diagram of PEMFC and (b) equivalent circuit diagram of PEMFC.

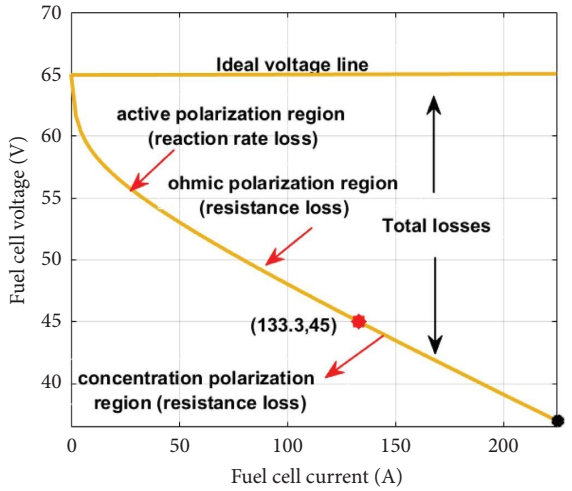

Figure 4: Nonlinear V-I characteristics of the PEMFC.

Table 1: Designed parameters of the polymer membrane fuel stack for the electric vehicle system.

Parameters	Values
Actual power supply rating of the polymer fuel stack	5.99 kW
Nominal voltage at fuel stack operating point position (V_{MPP})	45.22 V
Nominal current at fuel stack operating point position (I_{MPP})	133.33 A
Fuel stack working open-circuited voltage (V_{OC})	65.01 V
Partially available oxygen pressure	1.0 bar
Partially available hydrogen pressure	1.5 bar
Available fuel cells in the entire stack (n)	65.0
Rate of air flowing at the nominal operating point of the fuel stack (I_{pm})	506.4
The gasses constant parameter of the PEMFS (R)	84.1021 ($J \cdot mol^{-1} \cdot K^{-1}$)
Faraday constant of the polymer membrane fuel stack (F)	91,551.832 ($C \cdot mol^{-1}$)
Available oxidant composition of the fuel stack	21%
Total fuel composition of the fuel stack	99.88%
Total hydrogen composition of the fuel stack	99.77%
Overall usage of oxygen in the PEMFS	64.55%

$$P_{H_2} = \frac{1}{2}\mathrm{RH}_A P_{H_2O}^{\mathrm{sat}}\left(\frac{1}{\left(\mathrm{RH}_A * P_{H_2O}^{\mathrm{sat}}/P_A\right)\exp\left(1.6\left(I_{\mathrm{cell}}/A\right)/T_F\right)}\right), \tag{7}$$

$$P_{O_2} = \frac{1}{2}\mathrm{RH}_C P_{H_2O}^{\mathrm{sat}}\left(\frac{1}{\left(\mathrm{RH}_C P_{H_2O}^{sat}/P_C\right)\exp\left(4.1\left(I_c/A\right)/1.33 * T_F\right)}\right), \tag{8}$$

where E_{Octv}, V_0, V_C, and V_A are the thermodynamic, ohmic, concentrative, and active region voltages. Similarly, T_F is the fuel stack operating temperature. The partial hydrogen and partial oxygen parameters of the fuel stack are defined as P_{H_2} and P_{O_2}. The parameters RH_C and RH_A are the relative humidity vapor of the cathode and anode of the fuel stack. Finally, the P_{Ano} and P_{Cat} are defined as the anode and cathode inlet pressures. The fuel cell electrode area and its generated current are represented as "A" and "I_{cell}." The water vapor of the fuel stack is represented as $P_{H_2O}^{\mathrm{sat}}$. The fuel stack polarization voltages are obtained by using the following equation:

$$V_A = K_1 + K_2 * T_F + \left(K_3 + K_4\right) * T_F * \log\left(C_{O_2} + I_{\mathrm{cell}}\right), \tag{9}$$

$$V_C = -\frac{R * T_F}{n * F}\log\left(1 - \frac{i}{i_{\max}}\right), \tag{10}$$

$$V_O = I_{\mathrm{cell}} * \left(R_{\mathrm{ef}} + R_{\mathrm{pf}}\right), \tag{11}$$

where K_1, K_2, K_3, and K_4 are the utilized empirical coefficients and R is the total resistance of the fuel stack. Here, "i" is considered as the current density of the fuel stack. The Faraday constant and equivalent resistance of the anode and cathode are represented as "F," R_{ef}, and R_{pf}. The electrode area and relative permeability of the fuel stack are A and Φ_{ef}. The parameter C_{O_2} is the concentrated oxygen which is derived as follows:

$$C_{O_2} = \frac{P_{O_2}}{5.099e^6 \exp\left(-498/T_F\right)}, \tag{12}$$

$$i = \frac{I_{\mathrm{cell}}}{A}, \tag{13}$$

$$R_{\mathrm{ef}} = \frac{\Phi_{\mathrm{ef}} * Q}{A}, \tag{14}$$

$$\Phi_{\mathrm{ef}} = \frac{181.6\left[1 + 0.03i + 0.62\left(T_F/(303)^2\right) * i^{2.5}\right]}{(W - 0.634 - 3j) * \exp\left(4.18\left(T_F - 303\right)/T_F\right)}. \tag{15}$$

3. Design and Analysis of Hybrid MPPT Controllers

In this work, an adaptive genetic algorithm with an adaptive neuro-fuzzy inference system (ACS with ANFIS) MPPT controller is introduced for finding the MPP of the fuel stack system thereby extracting the peak power from the fuel cell. The proposed hybrid maximum power point tracking (MPPT) controller is compared with the other MPPT controllers which are enhanced incremental conductance-fuzzy logic controller (EIC with FLC), improved hill climb with fuzzy logic controller (IHC with FLC), adaptive beta with FLC, enhanced differential evolutionary with FLC (EDE with FLC), and marine predators optimization-FLC (MPO with FLC).

3.1. Hill Climb Optimized Fuzzy Logic MPPT Controller. So, in [50–52], the authors utilized the hybridization of the HC and fuzzy controller to enhance the working behavior of the fuel stack. Here, the HC and fuzzy controllers' drawbacks are neglected. At the start, the hill climb methodology is used for optimizing the tracking time of the MPP. After that, the HC is used to select the proper membership functions of the fuzzy controller. After selecting the suitable membership functions, the fuzzy is applied to the fuel stack system to remove the oscillations across the MPP. The features of this hybrid controller are easy to implement, less cost for manufacturing, moderate tracking speed, and good steady-state response. The error (e) and change of error (Δe) parameters are determined by using the equations (17) and (18). The changes in fuel stack power and variation of fuel stack currents are fed to the fuzzy network for generating the switching pulses to the DC-DC converter to improve the voltage rating of the fuel stack supply. The functioning point of the fuel stack does not reach the actual MPP position. So, the variable power ΔP moves through the gain controller to stabilize the functioning point of the fuel stack. Here, the fuzzy inputs are converted into four fuzzy sets which are identified as negative small (NS), negative big (NB), positive small (PS), and positive big (PB).

$$\begin{aligned} e(v) &= \frac{\Delta P_{\mathrm{FC}}}{\Delta V_{\mathrm{FC}}} \\ &= \frac{P_{\mathrm{FC}}(v) - P_{\mathrm{FC}}(v-1)}{V_{\mathrm{FC}}(v) - V_{\mathrm{FC}}(v-1)}, \end{aligned} \tag{16}$$

$$\Delta e(v) = \frac{\Delta P_{\mathrm{FC}}}{\Delta V_{\mathrm{FC}}} - e(v-1), \tag{17}$$

$$D(v) = \Delta D(v) - D(v-1), \tag{18}$$

where $P_{\mathrm{FC}}(v-1)$, $P_{\mathrm{FC}}(v)$, $V_{\mathrm{FC}}(v-1)$, and $V_{\mathrm{FC}}(v)$ are the past and present fuel stack powers and voltages. The converter present and previous converter duty cycles are $D(v)$ and $D(v-1)$.

3.2. Improved Differential Evolutionary-Based Fuzzy Logic MPPT Controller. The differential evolutionary algorithm works based on the fitness function. The fitness value is used to optimize the required objective function. Here, the population size is selected based on the lower and upper generation limits. In this algorithm, the mutation value is adjusted to obtain the best optimal value from all particles, and also, it gives a very good convergence speed. Also, this

algorithm solves all the nonlinearity problems of the fuel stack systems under different environmental conditions [53]. However, this algorithm requires a greater number of iterations for maintaining the constant fuel stack power. So, the research scholars hybridized the differential algorithm with the fuzzy logic controller to improve the overall system working efficiency. Here, the differential evolutionary algorithm is used for the final selection of the fuzzy membership functions. The membership functions are selected based on the iterative optimization process. As a result, the degree of freedom is applied to the fuzzy controller to track the functioning point of the polymer membrane fuel stack with high accuracy. The operational rules of the fuzzy system are given in Table 2. Here, the fuel stack current and fuel stack voltages are fed to the fuzzy block by utilizing the voltage sensor and current sensor. Here, the reference fuel stack voltages and fuel stack currents are compared with the actual voltage and currents to generate the error signal which is forwarded to the fuzzy block for generating the switching signals to the DC-DC converter. The error, change of error, and duty signal membership parameters are defined as L_1 to L_7, M_1 to M_7, and N_1 to N_7. Here, there are seven membership functions involved in the fuel stack input and output parameters which are zero state (S_0), positive state (S_1), positive state (S_2), positive state (S_3), negative state (S_1), negative sate (S_2), and negative sate (S_3).

3.3. Adaptive Beta Optimized Fuzzy Logic MPPT Controller. For designing the fuzzy membership functions, there are many experts required [54]. Here, the adaptive beta concept is applied to the fuzzy network for selecting proper membership functions to enhance the dynamic response of the fuel stack system. Here, the fuel stack constraints are maintained as constant, and the beta (β) variable is varied until the fuel stack reaches the actual maximum power point of the system. In this hybrid method, initially, β is used to move the functioning point of the fuel stack near the actual MPP position with different step size values. As a result, this hybrid controller's MPP tracking speed is increased extensively. The value of beta is decided by using equation (20). Later, the fuzzy controller starts working with the help of the beta method to reduce the distortions of the converter output voltages with small step size values. Here, the max-min and center of gravity methodologies are applied to the fuzzy network for the fuzzification process.

$$\beta(a) = \log\left(\frac{I_{\mathrm{FC}}}{V_{\mathrm{FC}}}\right) - N * V_{\mathrm{FC}}. \tag{19}$$

3.4. Enhanced Incremental Conductance-Fed Fuzzy Logic MPPT Controller. From the literature review, the conventional P&O methodologies are not utilizable because of the high steady-state oscillations across the functioning point of the fuel stack. Also, it gives high power conduction losses of the fuel stack system at the time of P&O method perturbation. So, the IC controller is utilized in the fuzzy logic network for improving the efficiency of the fuel stack-fed electric vehicle systems [55]. Similar to the previous techniques, in this hybrid IC with a fuzzy MPPT controller, at the start, the differential step constant is utilized in the IC method for moving the functioning point of the fuel stack at the actual MPP position with high speed. As a result, the overall controller convergence time is reduced. Here, the change of fuel stack power and voltages are indicated as $\mathrm{dP_{FC}}$ and $\mathrm{dV_{FC}}$. The fuel stack's present slope (X_P) and previous slope step ($X_{T-\mathrm{old}}$) values are supplied to the fuzzy controller in order to generate the new step value which is represented as ($X_{T-\mathrm{ew}}$). Based on all these slope values, the IC controller generates the duty pulses to the DC-DC converter for enhancing the voltage profile of the fuel stack system. Here, the fuzzy block consists of three types of stages which are named as low stage (LS), moderate stage (MS), and high stage (HS).

3.5. Marine Predators Optimized Fuzzy Logic-Based MPPT Controller. The modified marine predator's algorithm is used in [56] for solving the nonlinear issue of the electric vehicle system. This technique requires a greater number of iterations to find the required objective of the system. As a result, this controller generates voltage distortions in the converter output power. In addition, this controller needed more convergence time and was useful only for static working water membrane conditions of the fuel stack. Similarly, a fuzzy system alone is used in the renewable energy system for tracking the functioning point of the hybrid PV and fuel stack system. However, this fuzzy controller needed good skilled persons to design the membership functions. So, the current researchers developed the hybridized marine predator-based fuzzy system for enhancing the efficiency of fuel cell-based automotive systems. Here, the algorithm starts functioning with a marine predator controller for controlling the functioning point of the fuel stack from the initial position of the V-I curve to the actual MPP position. Once the PEMFS operating point reaches the required position of the V-I curve, then the fuzzy logic starts to reduce the oscillations across the fuel stack MPP. In this fuzzy controller, there are two input variables and one output variable which are fuel stack voltage, current, and converter duty cycle. These variables involve seven different fuzzy levels which are zero state (S_0), positive state (S_1), positive state (S_2), positive state (S_3), negative state (S_1), negative state (S_2), and negative state (S_3). Based on these seven fuzzy levels, there are 49 rules exist in the fuzzy network as shown in Table 3. These 49 rules smooth the fuel stack output voltage with less implementation cost. Finally, in the fuzzy logic system, the defuzzification process is used to adjust the duty cycle of the boost converter until reaching the actual MPP. The MPS with FLC-based MPPT controller absolute error and converter duty cycle updating have been carried out by using the following equations:

Table 2: Rules of the fuzzy membership functions between the fuel stack parameters.

Input membership functions		Change of error (Δe)						
		Neg_S_3	Neg_S_2	Neg_S_1	Zero_S_0	Pos_S_1	Pos_S_2	Pos_S_3
Error (e)	Neg_S_3	Neg_S_3	Neg_S_3	Neg_S_3	Neg_S_3	Neg_S_2	Neg_S_1	Zero_S_0
	Neg_S_2	Neg_S_3	Neg_S_3	Neg_S_3	Neg_S_2	Neg_S_1	Zero_S_0	Pos_S_1
	Neg_S_1	Neg_S_3	Neg_S_3	Neg_S_2	Neg_S_1	Zero_S_0	Pos_S_1	Pos_S_2
	Zero_S_0	Neg_S_3	Neg_S_2	Neg_S_1	Zero_S_0	Pos_S_1	Pos_S_2	Pos_S_3
	Pos_S_1	Neg_S_2	Neg_S_1	Zero_S_0	Pos_S_1	Pos_S_2	Pos_S_3	Pos_S_3
	Pos_S_2	Neg_S_1	Zero_S_0	Pos_S_1	Pos_S_2	Pos_S_3	Pos_S_3	Pos_S_3
	Pos_S_3	Zero_S_0	Pos_S_1	Pos_S_2	Pos_S_3	Pos_S_3	Pos_S_3	Pos_S_3

Table 3: Rules of the fuzzy membership functions between the fuel stack parameters.

Input membership functions		Change of error (Δe)						
		Neg_S_3	Neg_S_2	Neg_S_1	Zero_S_0	Pos_S_1	Pos_S_2	Pos_S_3
Error (e)	Neg_S_3	Neg_S_3	Neg_S_3	Neg_S_3	Zero_S_0	Pos_S_1	Pos_S_2	Zero_S_0
	Neg_S_2	Neg_S_3	Neg_S_2	Neg_S_2	Zero_S_0	Pos_S_1	Pos_S_2	Pos_S_1
	Neg_S_1	Neg_S_2	Neg_S_2	Neg_S_1	Zero_S_0	Pos_S_1	Pos_S_1	Pos_S_2
	Zero_S_0	Zero_S_0	Zero_S_0	Zero_S_0	Zero_S_0	Zero_S_0	Zero_S_0	Zero_S_0
	Pos_S_1	Pos_S_2	Pos_S_2	Pos_S_1	Zero_S_0	Neg_S_1	Neg_S_1	Neg_S_2
	Pos_S_2	Pos_S_3	Pos_S_2	Pos_S_2	Zero_S_0	Neg_S_2	Neg_S_2	Neg_S_3
	Pos_S_3	Pos_S_3	Pos_S_3	Pos_S_3	Zero_S_0	Neg_S_3	Neg_S_3	Neg_S_3

$$\text{Absolute error} = \int_{t=0}^{T_{\text{simu}}} \text{absol}\left(\frac{\mathrm{d}P_{\text{FC}}}{\mathrm{d}V_{\text{FC}}}\right) * \mathrm{d}t, \tag{20}$$

$$\text{Absolute error} = \int_{t=0}^{T_{\text{simu}}} \text{absol}\left(\frac{P_{\text{FC}(v)-}P_{\text{FC}(v-1)}}{V_{\text{FC}}(v) - V_{\text{FC}}(v-1)}\right) * \mathrm{d}t, \tag{21}$$

$$\Delta D(v) = \frac{\sum_{v=1}^{49} W_v * P_v}{\sum_{v=1}^{49} W_v}, \tag{22}$$

where "W" denotes the membership number for the particular rule v. Finally, P_V indicates the middle value of the particular membership function. The sampled duty signal is generated from the FLC and is compared with the saw-tooth signal with a particular frequency in order to generate the switching signals to the boost converter.

3.6. Proposed Adaptive Genetic Algorithm-Based ANFIS MPPT Controller. Maximum power point tracking is a very important task in power converter-fed renewable energy systems. Here, the fuel stack supplies fluctuated output power based on the operating temperature conditions, and its nonlinear behavior directly affects the performance of the fuel stack-dependent electric vehicle system. Here, the adaptive genetic algorithm-based ANFIS methodology is used to improve the power supply rating of the electric vehicle system. Here, the proposed controller works in three stages which are a determination of the optimum voltage of the fuel stack at different operating temperature conditions of the fuel stack, second one is the training of the ANFIS controller with the proper dataset, and the last one is the generation of the switching signals to the DC-DC converter. The backpropagation algorithm (BA) is used to obtain the dataset of the ANFIS controller. Due to this BP data training method, the ANFIS controller may track any local MPP of the fuel stack system at different working temperature conditions of the fuel stack. In this method, the AGA concept is used to train the datasets of the fuel stack system for generating the duty pulses to the boost converter by using the ANFIS methodology. The flowchart of the AGA-based ANFIS MPPT controller and its membership functions is shown in Figures 5 and 6. The drawbacks of this proposed algorithm are high complexity in design and more implementation cost which are compensated from the maximum power extraction of the fuel stack.

From Figure 6, the ANFIS controller consists of two supply variables which are u and v. Here, there are four membership function variables which are C_1, C_2, D_1, and D_2. In this hybrid method, the Takagi–Sugeno-dependent ANFIS methodology is used, and it consists of two rules which are mentioned in equations (23) and (24). From equation (23), the parameters c_i, d_i, and k_i are subsequent constants, and there are five layers in the ANFIS controller which are shown in Figure 6. Here, each layer node number is represented based on its related membership function, and the outputs of the 1-layer nodes are determined by using equations (25) and (26). From equation (25), the variables §; and $\mathrm{n}_{1,\mathrm{i}}$ are the utilized membership values for the corresponding supply variables u and v. Similarly, the parameters g and h are represented as membership values. Here, the efficiency of the MPPT controller is determined by using the fuel stack-generated power ($P_{\text{FC}} = V_{\text{FC}} * I_{\text{FC}}$) concerning the load power ($P_0 = V_0 * I_0$).

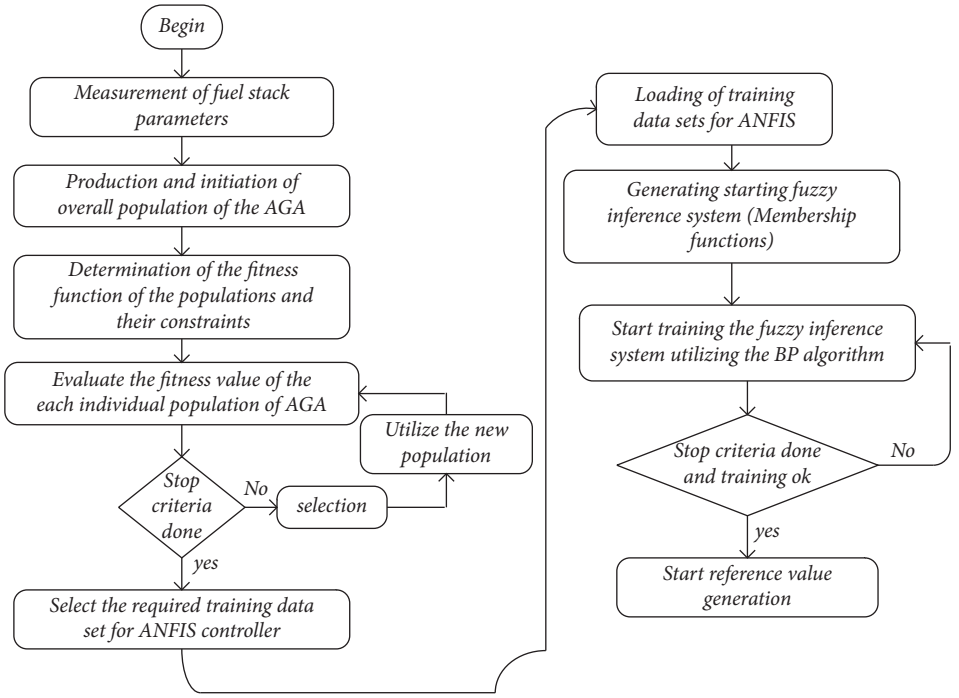

Figure 5: Proposed adaptive genetic algorithm-optimized ANFIS MPPT controller.

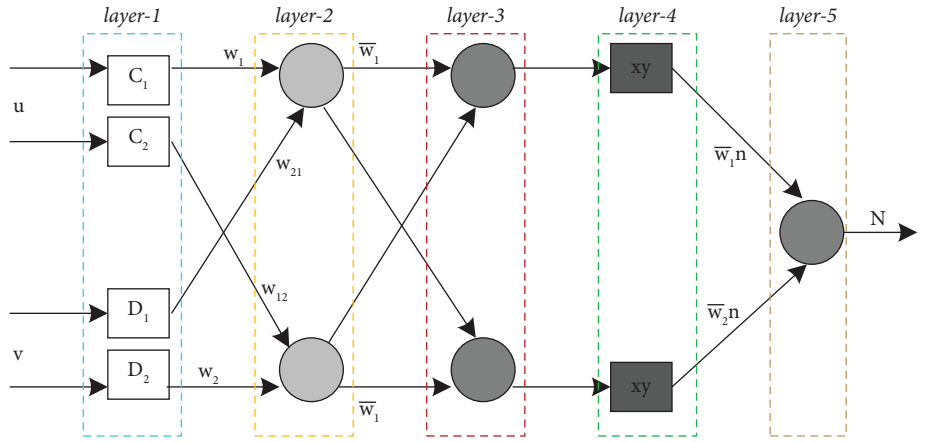

Figure 6: Adaptive genetic optimization-based ANFIS controller for PEMFS.

$$\text{if } u \text{ is } C_1, \text{and } v \text{ is } D_1 \text{ then } N = c_1 u + d_1 v + k_1, \tag{23}$$

$$\text{if } u \text{ is } C_2, \text{and } v \text{ is } D_2 \text{ then } N = c_2 u + d_2 v + k_2, \tag{24}$$

$$n_{1,i} = \S;_{C1}(u) + \S;_{C2}(u); \quad i = 1, 2 \cdots, \tag{25}$$

$$n_{1,i} = \S;_{D1}(v) + \S;_{D2}(v); \quad i = 1, 2 \cdots, \tag{26}$$

$$\S;_c(u) = \frac{1}{1 + |u - W_i/g_i|^{2h_i}}, \tag{27}$$

$$n_{2,i} = w_i = \S;_{c,k}(u) * \mu_{d,i}(v); \quad i = 1, 2, \tag{28}$$

$$n_{3,i} = w_i^T = \frac{w_i}{w_1 + w_2}; \quad i = 1, 2, \tag{29}$$

$$o_{4,i} = w_i * n_i = w_i^T (c_i u + d_i v + k_i); \quad i = 1, 2, \tag{30}$$

$$o_{5,i} = \sum_i w_i^T z_i = \frac{\sum_i w_i * z_i}{w_i}; \quad i = 1, 2. \tag{31}$$

4. Design and Analysis of Boost DC-DC Converter

All of the fuel stacks supply less amount of voltage which is not a desirable power supply for any electric vehicle application. So, the power DC-DC converter is used to improve the power supply rating of the fuel stack systems. Here, the nonisolated methodology is used in the power converter to reduce the implementation cost of the system. The selected conventional converter does not require any additional rectifier and transformer to enhance the system performance. So, the overall fuel stack-based power supply system switching and conduction losses are reduced. The features of a boost converter are optimal in size, less complexity in design, more lifetime, good flexibility, and high efficiency. Also, this converter involves very less components. The working structure of the utilized converter is given in Figures 7(a)–7(c). The voltage gain of the converter is derived as follows:

$$V_{\mathrm{FC}} * T_k * D + \left(V_{\mathrm{FC}} - V_0\right) * T_k * (1 - D) = 0, \tag{32}$$

$$-I_0 * D * T_k + (1 - D) * \left(I_{\mathrm{FC}} - I_0\right) * T_k = 0, \tag{33}$$

$$V_0 = \frac{V_{\mathrm{FC}}}{(1 - D)}, \& I_0 = I_{\mathrm{FC}} * (1 - D), \tag{34}$$

$$\frac{V_0}{I_0} = R_0, \& \frac{V_{\mathrm{FC}}}{I_{\mathrm{FC}}} = R_{\mathrm{FC}}, \tag{35}$$

where the parameters D, T_k, V_{FC}, and I_{FC} are represented as converter duty cycle, switching time duration, fuel stack voltage, and current. The operational waveforms of the converter are given in Figure 8.

5. Analysis of Simulation Results

The proposed system is designed by utilizing the MATLAB/Simulink software. Here, the polymer membrane fuel stack is selected for the analysis of the proposed MPPT controller along with the different other MPPT controllers. The advantages of this fuel stack are less corrosion issues and very less electrolyte handling problems. Also, it is capable of operating at very low temperatures and a very short starting time. Due to these features, it is used in most of the backup and portable charging systems. The design of the utilized fuel stack is given in Table 1. The major issue of any fuel system is more supply current which is optimized by using the various power converters.

Here, the boost power conversion circuit is used to reduce the fuel stack supply current. The utilized supply-side capacitor (C_{FC}) value is 120 μF which is useful for stabilizing the fuel power source and limiting the sudden changes in the source voltage. Similarly, the inductor (L_{FC}) value selected for the design of the DC-DC power converter is 1.28 mH. Here, the metal oxide field effect transistor (MOSFET) switch is utilized because of the very low switch ON resistance, and it works for high supply voltage applications. The consumer-side capacitor (C_g) selected value is 240 μF which manages the load voltage fluctuations within the minimum value. Finally, the utilized load resistor value is 88 Ω. Here, the entire system is investigated at various functioning temperature conditions of the PEMFS as mentioned in Figure 9.

The proposed power converter followed fuel stack network duty signal is produced by employing several MPPT techniques which are EIC with FLC, IHC with FLC, AB with FLC, EDE with FLC, MPO with FLC, and AGA with ANFIS controller. The obtained fuel stack and converter output parameters are given in Figure 10. From Figure 10(a), the PEMFS supplies the current and voltage by employing the AB with FLC, EDE with FLC, MPO with FLC, and AGA with ANFIS MPPT controllers at 303 K is 105.05 A, 37.27 V, 105.32 A, 37.35 V, 105.76 A, 37.42 V, 106.22 A, and 37.88 V,

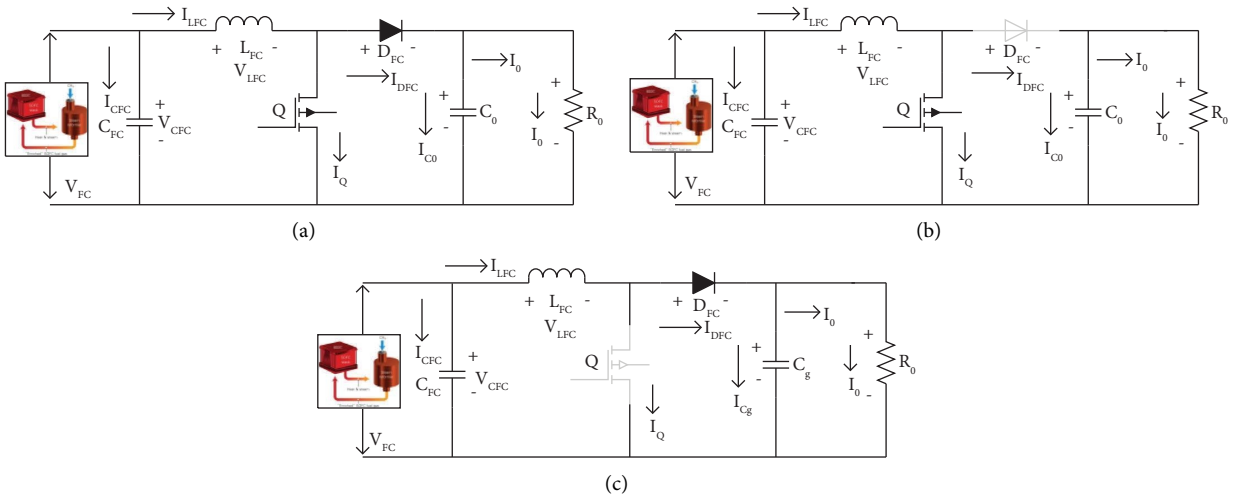

Figure 7: Conventional converter: (a) basic operation, (b) switching condition, and (c) blocking state of the switch.

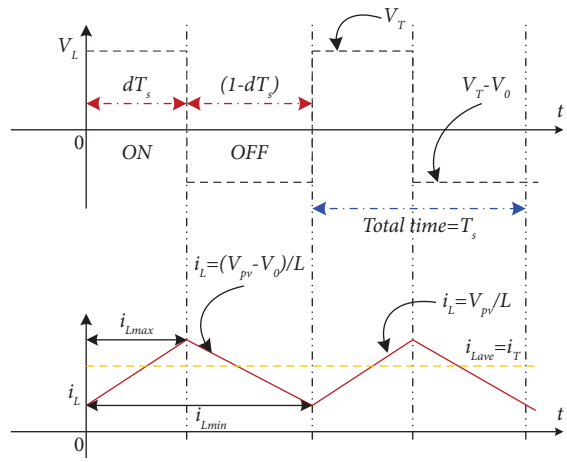

Figure 8: Converter duty signal and inductor charging currents.

respectively. Similarly, at the same functioning temperature, the converter current and voltages are 7.699 A, 498.87 V, 7.750 A, 499.12 V, 7.831A, 499.51 V, 7.851 A, and 499.95 V, respectively. The fuel stack produced voltage and powers by employing EIC with FLC and IHC with FLC are given in Figures 10(b) and 10(c). From Figure 10(d), the utilized power DC-DC converter increases the supply voltage of the fuel stack from 37.88 V to 499.95 V by employing the AGA-based ANFIS controller at 303 K temperature. Similarly, the DC-DC converter decreases the supply current levels from 105.76 A to 7.831 A by selecting the MPO with the FLC technique at 303 K temperature.

Finally, the collected load voltage and powers are given in Figures 10(e) and 10(f). Similarly, if the working temperature of the fuel stack is 323 K, then the power production from the overall network is quite high when equated to the previously selected temperature of the fuel stack. The recorded power, voltage, and current values of the fuel stack at 323 K by employing the AGA with ANFIS, MPO with FLC, EDE with FLC, AB with FLC, IHC with FLC, and EIC with FLC MPPT controllers are 4643.70 W, 41.27 V, 112.52 A, 4498.81 W, 40.05 V, 112.33 A, 4399.30 W, 39.22 V, 112.17 A, 4339.24 W, 38.91 V, 111.52 A, 4184.57 W, 37.89 V, 110.44 A, 4159.37 W, 37.84 V, and 109.92 A respectively. Similarly, the AGA with ANFIS controller generates very less distortions in the converter output voltage along with the suitable duty cycle of 0.62. The proposed system's working efficiency by employing AGA with ANFIS and MPO with FLC controllers at 323 K is 98.25% and 98.22%. Finally, the settling time duration of the AGA with ANFIS, MPO with FLC, EDE with FLC, AB with FLC, IHC with FLC, and EIC with FLC MPPT controllers is 0.0212 sec, 0.022 sec, 0.024 sec, 0.029 sec, 0.031 sec, and 0.032 sec. Similarly, other variations of fuel stack temperature and the waveforms of the PEMFS and converter are given in Figures 11 and 12. Finally, the detailed investigation of the proposed system is illustrated in Table 4.

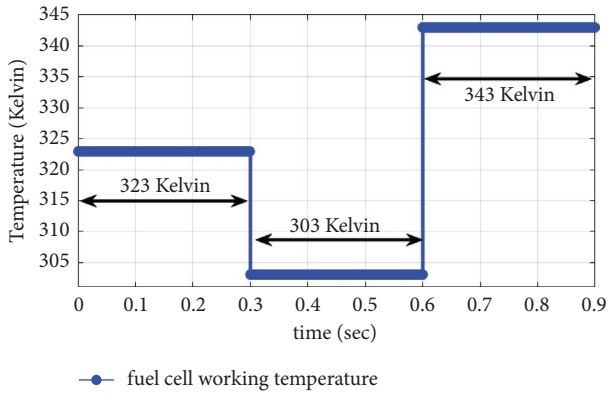

Figure 9: Functioning temperature of the polymer membrane fuel stack.

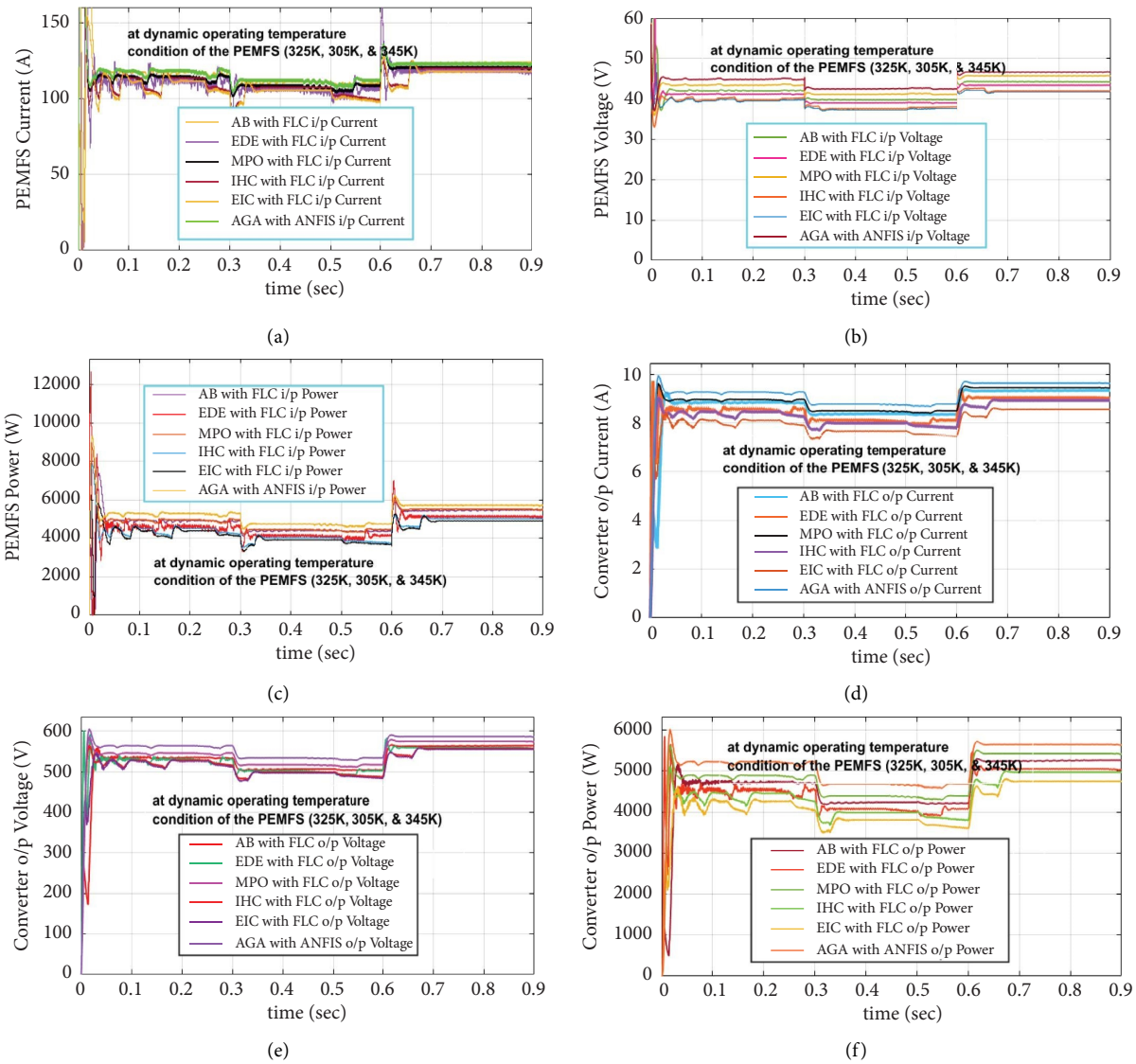

Figure 10: Fuel stack supplies: (a) current, (b) PEMFS voltage, (c) power of fuel stack, (d) converter current, (e) voltage of converter, and (f) power of converter at 323 K, 303 K, and 343 K.

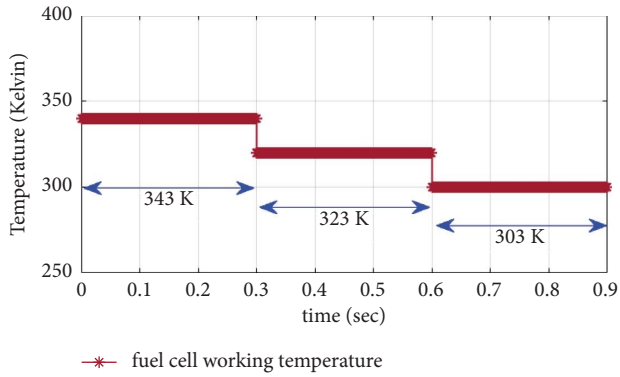

Figure 11: Temperature variation of the polymer membrane fuel stack.

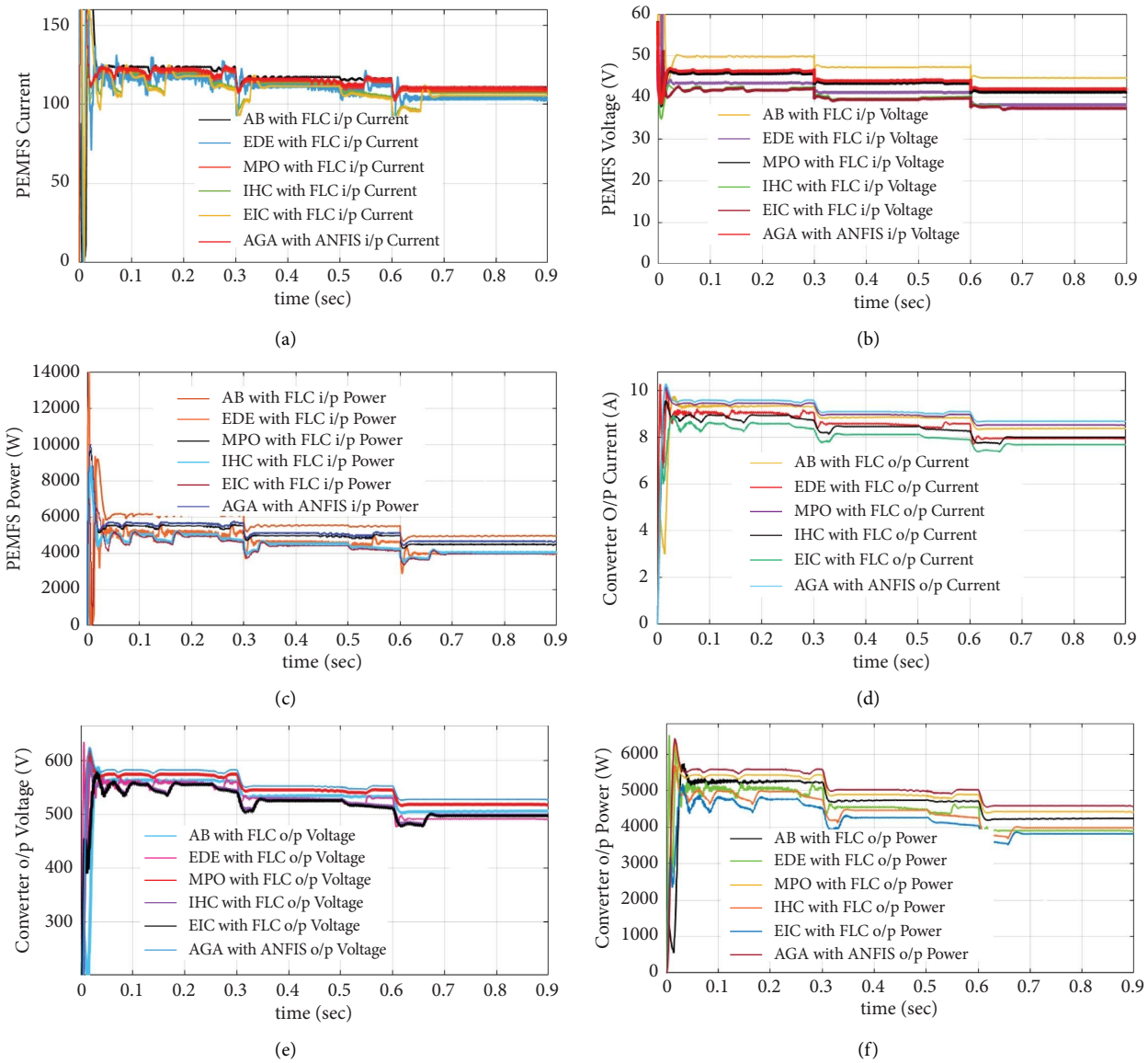

Figure 12: Fuel stack supplies: (a) current, (b) PEMFS voltage, (c) power of fuel stack, (d) converter current, (e) voltage of converter, and (f) power of converter at 343 K, 323 K, and 303 K.

Table 4: Recorded parameters of the fuel stack at diverse functioning temperature conditions.

Category of controller	Current of FS (A)	Voltage of FS (V)	Power of FS (W)	DC-DC current (A)	DC-DC voltage (V)	DC-DC power (W)	Efficiency (%)	Time of settling (sec)	Distortions
The functioning temperature of the fuel stack (303 K)									
EIC-FLC	104.20	36.14	3765.78	7.524	498.21	3585.775	95.22	0.042	High
IHC-FLC	104.89	36.92	3872.53	7.612	498.35	3711.43	95.84	0.038	High
AB-FLC	105.05	37.27	3915.21	7.699	498.87	3797.36	96.99	0.032	Medium
EDE-FLC	105.32	37.35	3933.70	7.750	499.12	3820.40	97.12	0.028	Medium
MPO-FLC	105.76	37.42	3957.53	7.831	499.51	3858.59	97.50	0.025	Low
AGA-ANFIS	106.22	37.88	4023.61	7.851	499.95	3931.46	97.71	0.021	Low
The functioning temperature of the fuel stack (323 K)									
EIC-FLC	109.92	37.84	4159.37	8.12	499.16	4047.898	97.32	0.032	High
IHC-FLC	110.44	37.89	4184.57	8.92	500.51	4076.18	97.41	0.031	High
AB-FLC	111.52	38.91	4339.24	8.95	501.23	4229.89	97.48	0.029	Medium
EDE-FLC	112.17	39.22	4399.30	8.98	501.32	4320.55	98.21	0.024	Medium
MPO-FLC	112.33	40.05	4498.81	8.99	501.88	4418.73	98.22	0.022	Low
AGA-ANFIS	112.52	41.27	4643.70	9.012	501.92	4562.435	98.25	0.0212	Low
The functioning temperature of the fuel stack (343 K)									
EIC-FLC	112.35	41.52	4664.77	8.96	501.90	4585.93	98.31	0.025	High
IHC-FLC	112.48	41.54	4672.41	8.99	501.98	4595.31	98.35	0.018	High
AB-FLC	113.08	41.50	4692.82	9.08	502.21	4616.32	98.37	0.0157	Medium
EDE-FLC	113.09	42.23	4775.79	9.09	502.24	4700.33	98.42	0.015	Medium
MPO-FLC	113.10	42.33	4787.52	9.18	502.25	4718.100	98.55	0.012	Low
AGA-ANFIS	113.11	42.34	4789.07	9.24	503.21	4720.58	98.57	0.010	Low

6. Conclusion

The AGA with ANFIS hybrid power point tracking controller is analyzed successfully along with the other recently existing hybrid MPPT controllers by employing the MATLAB/Simulink tool. Here, in the first objective, the PEMFS is utilized as a source for the electric vehicle application to produce a continuous power supply to the EV system with very few voltage distortions. The features of this fuel stack are rapid response and very little time for functioning. Also, it works for low and high operating temperature values of the fuel stack. In the second objective, the DC-DC power converter is employed for reducing the fuel stack-generated current. As a result, the entire proposed system works efficiently with very few conduction power losses. The advantages of this converter are simple in design and need fewer components for implementation. Finally, the major focus of this work is the development of an adaptive genetic algorithm-optimized ANFIS controller for extracting the maximum power from the fuel stack. Here, the AGA-based ANFIS controller generates the switching pulses to the DC-DC converter. The features of this proposed controller are good tracking speed, few oscillations across the MPP, few iterations of the GA to select the ANFIS membership functions, less converter output voltage fluctuations, and good dynamic response.

Nomenclature

MPPT: Maximum power point tracking
VSHC with FLC: Variable step hill climb optimized fuzzy logic controller
RBFN: Radial basis functional network
DE with FLC: Improved differential evolutionary with FLC
AB with FLC: Adaptive beta with FLC
GA with FLC: Genetic algorithm-optimized FLC
MPS with FLC: Marine predators optimized FLC
MOSFET: Metal oxide semiconductor field effect transistor
PAFC: Phosphoric acid fuel cell
ACS with ANFIS: Cuckoo search optimized adaptive neuro-fuzzy inference system
SOFC: Solid-oxide fuel cells
MCFC: Molten-carbonate fuel cells
PEMFC: Proton exchange membrane fuel cell.

Data Availability

The data used to support the findings of this study are included in the article.

Additional Points

Human Participants and/or Animals. This work does not affect any human beings or animals.

Ethical Approval

Authors are giving full ethical approval for publication.

Conflicts of Interest

The authors declare that they have no conflicts of interest.

Authors' Contributions

CH Hussaian Basha conceptualized the study, validated the study, performed formal analysis, investigated the study,

collected resources, and wrote the original draft of the manuscript. Ezzeddine Touti, Mouloud Aoudia, and Ibrahim Mohammed Alrougy wrote the review, edited the study, visualized the study, supervised the study, and administrated the project.

Acknowledgments

The authors extend their appreciation to the Deanship of Scientific Research at Northern Border University, Arar, KSA, for funding this research work through the project number "NBU-FFR-2024-1475-02."

References

[1] S. Belaid, D. Rekioua, A. Oubelaid, D. Ziane, and T. Rekioua, "Proposed hybrid power optimization for wind turbine/battery system," *Periodica polytechnica Electrical engineering and computer science*, vol. 66, no. 1, pp. 60–71, 2022.

[2] M. R. Negahdari, A. Ghaedi, M. Nafar, and S. Mohsen, "Optimal planning of the barrage type tidal power plants equipped to the hydro-pumps," *Electric Power Systems Research*, vol. 220, 2023.

[3] A. D. Sakti, P. Rohayani, N. A. Izzah et al., "Spatial integration framework of solar, wind, and hydropower energy potential in Southeast Asia," *Scientific Reports*, vol. 13, no. 1, p. 340, 2023.

[4] C. H. H. Basha and C. Rani, "Different conventional and soft computing MPPT techniques for solar PV systems with high step-up boost converters: a comprehensive analysis," *Energies*, vol. 13, no. 2, p. 371, 2020.

[5] C. H. Hussaian Basha and C. Rani, "Performance analysis of MPPT techniques for dynamic irradiation condition of solar PV," *International Journal of Fuzzy Systems*, vol. 22, no. 8, pp. 2577–2598, 2020.

[6] S. R. Kiran, C. H. Basha, V. P. Singh, C. Dhanamjayulu, B. R. Prusty, and B. Khan, "Reduced simulative performance analysis of variable step size ANN based MPPT techniques for partially shaded solar PV systems," *IEEE Access*, vol. 10, pp. 48875–48889, 2022.

[7] C. H. Basha and C. Rani, "Design and analysis of transformerless, high step-up, boost DC-DC converter with an improved VSS-RBFA based MPPT controller," *International Transactions on Electrical Energy Systems*, vol. 30, no. 12, 2020.

[8] C. H. Hussaian Basha, V. Bansal, C. Rani, R. M. Brisilla, and S. Odofin, "Development of cuckoo search MPPT algorithm for partially shaded solar PV SEPIC converter," *Soft Computing for Problem Solving: SocProS 2018*, Springer, Singapore, 2020.

[9] N. Mebarki, T. Rekioua, Z. Mokrani, and D. Rekioua, "Supervisor control for stand-alone photovoltaic/hydrogen/battery bank system to supply energy to an electric vehicle," *International Journal of Hydrogen Energy*, vol. 40, no. 39, pp. 13777–13788, 2015.

[10] Z. Mokrani, D. Rekioua, N. Mebarki, T. Rekioua, and S. Bacha, "Energy management of battery-PEM Fuel cells Hybrid energy storage system for electric vehicle," in *Proceedings of the 2016 International Renewable and Sustainable Energy Conference (IRSEC)*, IEEE, Marrakech, Morocco, November 2016.

[11] M. A. Abdelkareem, K. Elsaid, T. Wilberforce, M. Kamil, E. T. Sayed, and A. Olabi, "Environmental aspects of fuel cells: a review," *Science of the Total Environment*, vol. 752, 2021.

[12] Y. Belkhier, A. Oubelaid, and R. N. Shaw, "Hybrid power management and control of fuel cells-battery energy storage system in hybrid electric vehicle under three different modes," *Energy Storage*, vol. 6, no. 1, p. e511, 2023.

[13] A. A. A. Alahmadi, Y. Belkhier, N. Ullah et al., "Hybrid wind/PV/battery energy management-based intelligent non-integer control for smart DC-microgrid of smart university," *IEEE Access*, vol. 9, pp. 98948–98961, 2021.

[14] N. Russner, S. Dierickx, A. Weber, R. Reimert, and E. Ivers-Tiffée, "Multiphysical modelling of planar solid oxide fuel cell stack layers," *Journal of Power Sources*, vol. 451, 2020.

[15] C. Park, Y. Jung, K. Lim, B. Kim, Y. Kang, and H. Ju, "Analysis of a phosphoric acid fuel cell-based multi-energy hub system for heat, power, and hydrogen generation," *Applied Thermal Engineering*, vol. 189, 2021.

[16] A. A. Ahmed, H. F. Ramadhan, M. Emheisen et al., "Improving the performance of the electric vehicle suspension system using sliding mode controller and PID controller," in *Proceedings of the 2023 IEEE 3rd International Conference on Sustainable Energy and Future Electric Transportation (SEFET)*, IEEE, Bhubaneswar, India, August 2023.

[17] C. Wan, J. Jin, X. Wei et al., "Inducing the SnO2-based electron transport layer into NiFe LDH/NF as efficient catalyst for OER and methanol oxidation reaction," *Journal of Materials Science & Technology*, vol. 124, pp. 102–108, 2022.

[18] H. Zhang, S. Huang, M. Salla et al., "A redox-mediated zinc–air fuel cell," *ACS Energy Letters*, vol. 7, no. 8, pp. 2565–2575, 2022.

[19] Q. Zhang and J. Guan, "Applications of atomically dispersed oxygen reduction catalysts in fuel cells and zinc–air batteries," *Energy & Environmental Materials*, vol. 4, no. 3, pp. 307–335, 2021.

[20] D. Qiu, L. Peng, P. Yi, W. Lehnert, and X. Lai, "Review on proton exchange membrane fuel cell stack assembly: quality evaluation, assembly method, contact behavior and process design," *Renewable and Sustainable Energy Reviews*, vol. 152, 2021.

[21] D. Chen, P. Pei, Y. Li et al., "Proton exchange membrane fuel cell stack consistency: evaluation methods, influencing factors, membrane electrode assembly parameters and improvement measures," *Energy Conversion and Management*, vol. 261, 2022.

[22] A. Harrag and H. Bahri, "A novel single sensor variable step size maximum power point tracking for proton exchange membrane fuel cell power system," *Fuel Cells*, vol. 19, no. 2, pp. 177–189, 2019.

[23] M. İnci, "A flexible perturb & observe MPPT method to prevent surplus energy for grid-failure conditions of fuel cells," *International Journal of Hydrogen Energy*, vol. 46, no. 79, pp. 39483–39498, 2021.

[24] J. Y. Fam, S. Y. Wong, H. B. M. Basri, M. O. Abdullah, K. B. Lias, and S. Mekhilef, "Predictive maximum power point tracking for proton exchange membrane fuel cell system," *IEEE Access*, vol. 9, pp. 157384–157397, 2021.

[25] C. Zhou, Z. Y. Liu, Y. N. Sun, and L. Mao, "A novel maximum power point tracking technique with improved particle swarm optimization for proton exchange membrane fuel cell," *Journal of Physics: Conference Series*, vol. 2347, no. 1, 2022.

[26] C. H. H. Basha, C. Rani, and S. Odofin, "A review on non-isolated inductor coupled DC-DC converter for photovoltaic grid-connected applications," *International Journal of Renewable Energy Resources*, vol. 7, no. 4, pp. 1570–1585, 2017.

[27] A. Trivedi, A. Gupta, R. K. Pachauri, and Y. K. Chauhan, "Comparison of Perturb & Observe and Ripple correlation

control MPPT algorithms for PV array," in *Proceedings of the 2016 IEEE 1st International Conference on Power Electronics, Intelligent Control and Energy Systems (ICPEICES)*, IEEE, Delhi, India, July 2016.

[28] M. Derbeli, O. Barambones, M. Y. Silaa, and C. Napole, "Real-time implementation of a new MPPT control method for a DC-DC boost converter used in a PEM fuel cell power system," *Actuators*, vol. 9, no. 4, p. 105, 2020.

[29] M. Derbeli, O. Barambones, and L. Sbita, "A robust maximum power point tracking control method for a PEM fuel cell power system," *Applied Sciences*, vol. 8, no. 12, p. 2449, 2018.

[30] B. Tifour, M. Boukhnifer, A. Hafaifa, and C. Tanougast, "An optimal fuzzy logic control for a fuel cell hybrid electric vehicle based on particle swarm and advisor," in *Proceedings of the 2021 IEEE Green Technologies Conference (GreenTech)*, IEEE, Denver, CO, USA, April 2021.

[31] A. Oubelaid, H. Alharbi, A. S. B. Humayd, N. Taib, T. Rekioua, and S. S. Ghoneim, "Fuzzy-energy-management-based intelligent direct torque control for a battery—supercapacitor electric vehicle," *Sustainability*, vol. 14, no. 14, p. 8407, 2022.

[32] W. Ahmad, U. H. Khan, Z. A. Khan, I. U. Haq, Z. Alam, and R. Khan, "A novel neuro-fuzzy GmpptAlgorithm based on generalized global sliding mode concept for variable-shaded photovoltaic system," in *Proceedings of the 2020 International Conference on Emerging Trends in Smart Technologies (ICETST)*, IEEE, Karachi, Pakistan, March 2020.

[33] C. Makdisie, B. Haidar, and H. H. Alhelou, *An Optimal Photovoltaic Conversion System for Future Smart Grids. Handbook of Research on Power and Energy System Optimization*, IGI Global, Hershey, PY, USA, 2018.

[34] Y. Belkhier, A. Achour, R. N. Shaw, N. Ullah, M. S. Chowdhury, and K. Techato, "Fuzzy supervisory passivity-based high order-sliding mode control approach for tidal turbine-based permanent magnet synchronous generator conversion system," *Actuators*, vol. 10, no. 5, p. 92, 2021.

[35] S. Tamalouzt, Y. Belkhier, Y. Sahri, N. Ullah, R. N. Shaw, and M. Bajaj, "New direct reactive power control based fuzzy and modulated hysteresis method for micro-grid applications under real wind speed," *Energy Sources, Part A: Recovery, Utilization, and Environmental Effects*, vol. 44, no. 2, pp. 4862–4887, 2022.

[36] H. Abouobaida, Y. Mchaouar, Y. Abouelmahjoub, H. Mahmoudi, A. Abbou, and M. Jamil, "Performance optimization of the INC-COND fuzzy MPPT based on a variable step for photovoltaic systems," *Optik*, vol. 278, 2023.

[37] K. Kayisli, "Super twisting sliding mode-type 2 fuzzy MPPT control of solar PV system with parameter optimization under variable irradiance conditions," *Ain Shams Engineering Journal*, vol. 14, no. 1, 2023.

[38] C. Baştemur Kaya, "A novel hybrid method based on the marine predators algorithm and adaptive neuro-fuzzy inference system for the identification of nonlinear systems," *Symmetry*, vol. 15, no. 9, p. 1765, 2023.

[39] C. H. Basha and M. Murali, "A new design of transformerless, non-isolated, high step-up DC-DC converter with hybrid fuzzy logic MPPT controller," *International Journal of Circuit Theory and Applications*, vol. 50, no. 1, pp. 272–297, 2022.

[40] V. Govinda Chowdary, V. Udhay Sankar, D. Mathew, C. H. Hussaian Basha, and C. Rani, "Hybrid fuzzy logic-based MPPT for wind energy conversion system," *Soft Computing for Problem Solving: SocProS 2018*, Springer, Singapore, 2020.

[41] S. Ahmadi, S. Abdi, and M. Kakavand, "Maximum power point tracking of a proton exchange membrane fuel cell system using PSO-PID controller," *International Journal of Hydrogen Energy*, vol. 42, no. 32, pp. 20430–20443, 2017.

[42] S. Singh, V. K. Tayal, H. P. Singh, and V. K. Yadav, "Design of PSO-tuned FOPI & Smith predictor controller for nonlinear polymer electrolyte membrane fuel cell," *Energy Sources, Part A: Recovery, Utilization, and Environmental Effects*, pp. 1–22, 2022.

[43] R. Vinu and V. Paul, "Robust optimized artificial neural network based PEM fuelcell voltage tracking," in *Proceedings of the 6th International Conference on Innovations in Bio-Inspired Computing and Applications (IBICA 2015)*, Springer International Publishing, Kochi, India, December 2015.

[44] D. N. Luta and A. Raji, "Fuzzy rule-based and particle swarm optimisation MPPT techniques for a fuel cell stack," *Energies*, vol. 12, no. 5, p. 936, 2019.

[45] Z. Wang, J. Mao, Z. He, and F. Liang, "Fuzzy control based on IQPSO in proton-exchange membrane fuel-cell temperature system," *Journal of Energy Engineering*, vol. 146, no. 5, 2020.

[46] Y. Qin, G. Zhao, Q. Hua, L. Sun, and S. Nag, "Multiobjective genetic algorithm-based optimization of PID controller parameters for fuel cell voltage and fuel utilization," *Sustainability*, vol. 11, no. 12, p. 3290, 2019.

[47] A. S. Al-Araji, H. A. Dhahad, and E. A. Jaber, "A neural networks based predictive voltage-tracking controller design for proton exchange membrane fuel cell model," *Journal of Engineering*, vol. 25, pp. 26–48, 2019.

[48] T. Hai, J. Zhou, and K. Muranaka, "An efficient fuzzy-logic based MPPT controller for grid-connected PV systems by farmland fertility optimization algorithm," *Optik*, vol. 267, 2022.

[49] C. Hussaian Basha, M. Murali, S. Rafikiran, T. Mariprasath, and M. Bhaskara Reddy, "An improved differential evolution optimization controller for enhancing the performance of PEM fuel cell powered electric vehicle system," *Materials Today: Proceedings*, vol. 52, pp. 308–314, 2022.

[50] S. Rafikiran, G. Devadasu, C. H. Basha et al., "Design and performance analysis of hybrid MPPT controllers for fuel cell fed DC-DC converter systems," *Energy Reports*, vol. 9, pp. 5826–5842, 2023.

[51] A. Dida and D. B. Attous, "Adaptive hill-climb searching method for MPPT algorithm based DFIG system using fuzzy logic controller," *International Journal of System Assurance Engineering and Management*, vol. 8, no. S1, pp. 424–434, 2017.

[52] C. H. H. Basha and C. Rani, "A New single switch DC-DC converter for PEM fuel cell-based electric vehicle system with an improved beta-fuzzy logic MPPT controller," *Soft Computing*, vol. 26, no. 13, pp. 6021–6040, 2022.

[53] H. Rezk, M. Aly, and A. Fathy, "A novel strategy based on recent equilibrium optimizer to enhance the performance of PEM fuel cell system through optimized fuzzy logic MPPT," *Energy*, vol. 234, 2021.

[54] X. Li, H. Wen, Y. Hu, and L. Jiang, "A novel beta parameter based fuzzy-logic controller for photovoltaic MPPT application," *Renewable Energy*, vol. 130, pp. 416–427, 2019.

[55] K. H. Reddy, R. Vijayasanthi, and K. RamaSudha, "Modeling and performance analysis of perturb and observe (P&O) incremental conductance (IC) fuzzy logic and model predictive MPPT controllers using a boost converter," *International Journal of Innovative Science and Research Technology*, vol. 5, no. 12, pp. 59–67, 2020.

[56] E. H. Houssein, M. A. Mahdy, A. Fathy, and H. Rezk, "A modified Marine Predator Algorithm based on opposition based learning for tracking the global MPP of shaded PV system," *Expert Systems with Applications*, vol. 183, 2021.